JOURNAL OF PHYSICAL ORGANIC CHEMISTRY
J. Phys. Org. Chem. 2003; **16:** 336–347
Published online 2003 in Wiley InterScience (www.interscience.wiley.com). DOI: 10.1002/poc.634

Prediction of tautomeric preferences and pK_a values for oxyluciferin and its constituent heterocycles

Erin E. Dahlke and Christopher J. Cramer*

Department of Chemistry and Supercomputing Institute, University of Minnesota, 207 Pleasant St. SE, Minneapolis, Minnesota 55455-0431, USA

Received 23 January 2003; revised 21 February 2003; accepted 24 February 2003

ABSTRACT: Well converged electronic structure calculations are employed to predict the relative energies of tautomers of thiazol-5(4*H*)-one/5-hydroxythiazole. Benchmarks established for this system are then employed to correct less complete levels of theory applied to the prediction of relative tautomer energies in substituted cases, including oxyluciferin. In the gas phase and aqueous solution, weak preferences for hydroxy and keto tautomers, respectively, are generally observed, but the magnitude is such that mixtures containing significant quantities of minor tautomers are predicted in most instances. The first pK_a value for oxyluciferin is predicted to be 6.5, with phenolate tautomers dominating the anionic equilibrium. Copyright © 2003 John Wiley & Sons, Ltd.

KEYWORDS: oxyluciferin; tautomers; relative energy; pK_a; bioluminescence; firefly

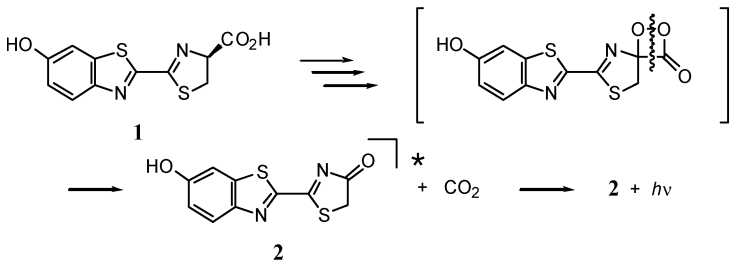

Scheme 1

INTRODUCTION

Fireflies are best known for their riveting bioluminescence. The mechanism of light generation is mediated by the enzyme luciferase, which oxidizes luciferin (**1**) to a dioxetanone that then fragments to CO_2 and a singlet excited state of oxyluciferin (**2**); the decay of the latter is responsible for photon emission (Scheme 1).[1–14]

Fascinatingly, the wavelength of the photon emitted from excited-state **2** can vary significantly as a function of firefly phenotype (with different luciferases known for different species) and, within a single phenotype, as a function of temperature, solvent or pH.[1,8,9,11,15–21] Emitted wavelengths can range from blue (430 nm) to red (635 nm); the familiar *in vivo* color that brightens a midsummer's evening is an intermediate yellow–green (562 nm). Variations in wavelength as a function of substitution of **2** (typically involving alkylation of the non-benzannelated thiazole ring, but not always) have also been reported.[8,18,21–24]

Three different effects have been proposed to influence the photoemission wavelength of excited-state **2**. First, with or without assistance from the luciferase enzyme, excited-state **2** may tautomerize from its thiazol-5(4*H*)-one form to its enol form (a 5-hydroxythiazole) prior to photoemission, thereby changing the nature of the emitting species. Second, the ionization state of **2** may be modified by pH and/or active site electrostatics, favoring deprotonation of either the phenolic hydroxyl group or the 4*H*-thiazole ring (or the hydroxythiazole hydroxyl group, if that tautomer is antecedent) or both (because of its instability in aqueous solution,[18] pK_a values for **2** are not known). Finally, the constraints of the luciferase active site in different phenotypes may be such that different torsion angles about the C—C bond joining the two heterocyclic components of **2** will be enforced, leading to different photophysics.

The application of molecular modeling techniques to

**Correspondence to:* C. J. Cramer, Department of Chemistry and Supercomputing Institute, University of Minnesota, 207 Pleasant St. SE, Minneapolis, Minnesota 55455-0431, USA.
E-mail: cramer@chem.umn.edu

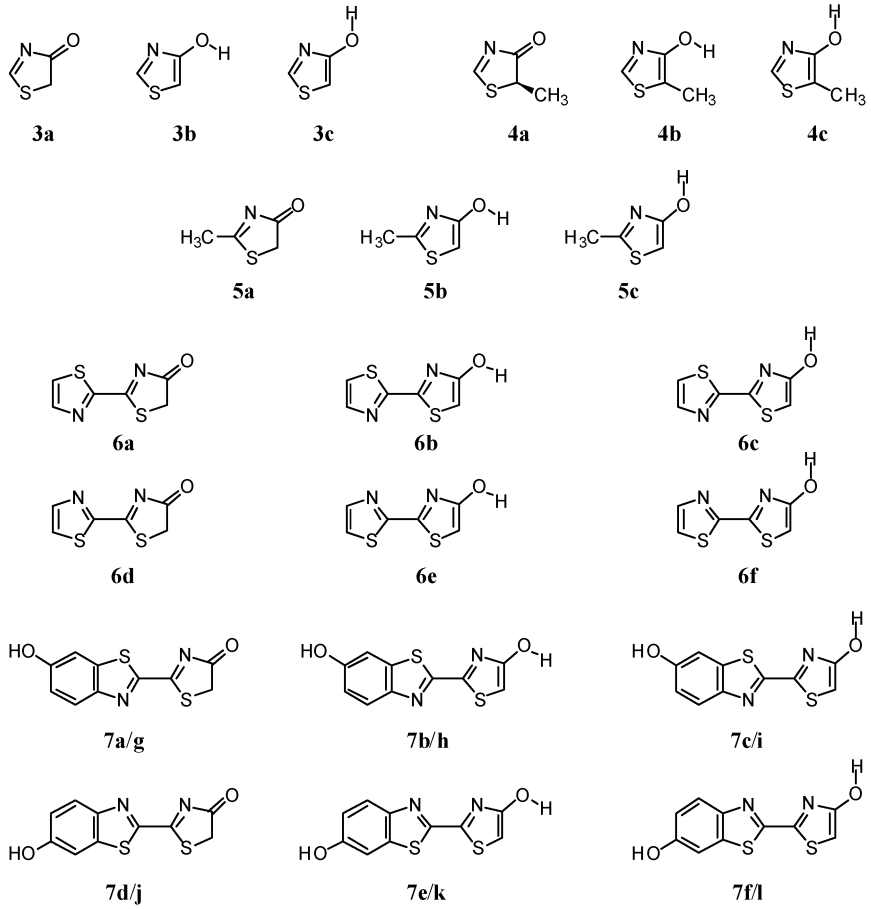

Scheme 2

the determination of free energy differences between tautomeric forms of heterocycles, both in the gas phase and in solution, has a long history,[25–35] in part deriving from early interest in the possible role of nucleic acid base tautomers in mutagenesis.[36,37] High accuracy for small heterocycles can typically be achieved with only a modest investment of computational resources, although larger systems can still pose challenges, since convergence of the relevant quantum mechanical equations with respect to basis set size and electron correlation becomes significantly more difficult. Prediction of pK_a values has also been a very active area of molecular modeling; in this instance high accuracy is more difficult to achieve from first-principles calculations, but empirical corrections to raw predictions can be useful.[28,33,38–46] In this work, we employ quantum mechanical methodologies to predict free energy differences between different tautomers and ionization states for ground-state oxyluciferin, its heterocyclic constituents and various alkylated analogs in both the gas phase and aqueous solution, in order to shed more light on the intrinsic energetics associated with these processes.

COMPUTATIONAL METHODS

Gas-phase calculations

The geometries for *all* structures were optimized at the hybrid Hartree–Fock density-functional level of theory[46] employing the gradient-corrected exchange and correlation functionals of Perdew and co-workers[47–49] as modified by Adamo and Barone[50] (*m*PW1PW91) in conjunction with the 6–31G(d) basis set.[51] All stationary points were verified as local minima by analytical frequency calculations, the data from which were also used to compute 298 K thermal contributions to gas-phase free energies using standard ideal-gas, rigid-rotor, harmonic-oscillator partition-function approximations.[46]

A number of other levels of theory were employed both for geometry optimizations and for single-point energy calculations on particular structures. Within a molecular orbital formalism,[46,51] these levels included Hartree–Fock theory, many-body perturbation theory through fourth order, coupled-cluster theory including single, double and triple excitations (the triples being perturbatively estimated), and the multi-coefficient quadratic-configuration interaction including singles

and doubles (MCQCISD)[52] and multi-coefficient G3 (MCG3)[53,54] methods of Truhlar and co-workers. Within a density functional formalism,[46,55] we also examined the pure and hybrid functionals known as BPW91, B3LYP and PBE1PBE. In connection with these calculations, a number of different basis sets[46,51] were considered, ranging in size for the DFT methods from MIDI![56] to aug-cc-pVTZ[57–59] and for the MCQCISD geometry optimizations and MCG3 calculations up to an improved version of the 6–311++G(3d2f,2df,2p) basis set.[52,60]

Aqueous solution calculations

Standard-state solvation free energies in water (dielectric constant $\epsilon = 78.3$) were calculated using the SM5.42R/BPW91/6–31G(d) aqueous solvation model[61] based on empirical atomic surface tensions and self-consistent reaction field calculations with CM2 class IV charges;[62] these calculations employed optimized gas-phase geometries (the R in SM5.42R implies that the model was designed to use gas-phase geometries kept rigid in the liquid solution phase). All calculations were carried out with a locally modified version of the Gaussian 98 electronic structure program suite.[63,64]

Software

MO and DFT calculations were carried out with the Gaussian 98 program suite,[63] as augmented with MN-GSM for SM5.42R calculations.[64] Multi-coefficient calculations employed the MULTILEVEL code.[65]

NOMENCLATURE

We consider a number of different heterocycles in this paper. Each heterocycle is identified by an Arabic numeral specific to its empirical formula and a roman letter specific to its tautomeric form (Scheme 2). We make an effort to preserve uniformity in nomenclature with respect to tautomeric form. Thus, for instance, **a** always refers to a keto tautomer incorporating a thiazol-5(4*H*)-one moiety, **b** to a 5-hydroxythiazole tautomer with the proton of the hydroxyl group antiperiplanar to the thiazole C(OH)—N bond and **c** to a 5-hydroxythiazole tautomer with the proton of the hydroxyl group antiperiplanar to the thiazole C(OH)═C bond. In the bisthiazole system **6**, an additional isomerism is associated with rotation about the 2,2′ bond joining the two heterocycles, giving rise to tautomers **d**–**f** that are otherwise equivalent to **a**–**c** (favorable π overlap enforces near co-planarity of the two rings, so no rotational isomers beyond these two are observed). Finally, in the oxyluciferin system **7**, each of the six possible tautomers analogous to those for **6** has an additional isomerism associated with rotation of the phenolic hydroxyl group. We find isomers related as phenolic rotamers to be very close to one another in energy, but for the sake of completeness, we label those having the hydroxyl proton oriented towards the side of the aromatic ring bearing the sulfur substituent of the thiazole ring as **a**–**f** and the alternative rotamers as **g**–**l**.

For the monoanion derived from deprotonation of **3**, no issues of isomerism arise, insofar as the proton that is lost is the one responsible for tautomerism; this species will be referred to simply as $\mathbf{3}^-$. The possible anions created by deprotonation of **7**, however, are more complex. Deprotonation of the phenol does not reduce opportunities for tautomerism in the non-benzannelated thiazole ring, nor for rotational isomerism about the bisthiazole bond. Thus, six isomers of the phenolate derived from **7** exist, and we refer to this collection at $^-$**7a**–$^-$**7f**; the negative charge symbol is placed to the left of the number because the phenol hydroxyl is to the left in all structures drawn in Scheme 2. Deprotonation of **7** at its other acidic position generates four additional anions, differing as *syn* and *anti* rotamers about the bisthiazole C—C bond and the phenolic C—O bond. We will refer to these structures as $\mathbf{7a}^-$, $\mathbf{7d}^-$, $\mathbf{7g}^-$ and $\mathbf{7j}^-$, where the two rotational angles in the anions are defined to be those found in the neutral **7** having the same roman letter and the negative charge symbol to the right emphasizes the position of deprotonation. Note, of course, that members of populations $^-$**7** and $\mathbf{7}^-$ are *all* related as tautomers, so a mixture of components of both may be present at equilibrium.

RESULTS AND DISCUSSION

Gas-phase tautomerism of neutral heterocycles

For **3**, the smallest heterocycle considered here, we evaluated relative tautomeric energies at many different levels of theory, in part in order to identify optimal choices for the larger cases, where computational compromises will have to be made. In the absence of available experimental results, we take the MCG3//MCQCISD level of theory as a standard, i.e. molecular geometries optimized at the multi-coefficient quadratic configuration interaction level including single and double excitations[52] and energies computed for those geometries at the multi-coefficient Gaussian-3 level.[53,54] This level of theory has been demonstrated to give agreement with experiment to within 1 kcal mol^{-1} (1 kcal = 4.184 kJ) for enthalpies of formation and reaction over a large body of data.[53,54,66]

Table 1 lists the relative tautomeric energies at different levels of theory for **3**, along with errors for other levels compared with MCG3//MCQCISD. Error is defined here simply as the mean of the absolute error in the tautomer energies predicted for **3b** and **3c** relative to **3a** when compared with MCG3//MCQCISD. Figure 1

Table 1. Gas-phase electronic energies and 298 K thermal contributions (kcal mol^{-1}) relative to **3a** at various levels of theory

		Relative energy[a]		
Level of theory	Geometry	**3b**	**3c**	Error
MCG3	MCQCISD	1.2	−2.1	
MP2/aug-cc-pVDZ	MP2/cc-pVDZ	1.1	−2.1	0.1
MP2/aug-cc-pVTZ	PBE1PBE/6–31G(d)	1.2	−2.0	0.1
MP2/aug-cc-pVTZ	*m*PW1PW91/6–31G(d)	1.3	−2.0	0.2
MP2/aug-cc-pVTZ	B3LYP/6–31G(d)	1.3	−1.9	0.2
PBE1PBE/aug-cc-pVTZ	B3LYP/6–31G(d)	1.7	−1.6	0.6
PBE1PBE/aug-cc-pVTZ	*m*PW1PW91/cc-pVTZ	1.7	−1.6	0.6
*m*PW1PW91/aug-cc-pVTZ	B3LYP/6–31G(d)	2.1	−1.2	1.0
*m*PW1PW91/aug-cc-pVTZ	*m*PW1PW91/cc-pVTZ	2.1	−1.2	1.0
MP2/cc-pVDZ	MP2/cc-pVDZ	2.3	−0.9	1.2
*m*PW1PW91/cc-pVTZ	*m*PW1PW91/cc-pVTZ	2.4	−0.9	1.3
PBE1PBE/cc-pVTZ	PBE1PBE/cc-pVTZ	2.1	0.0	1.6
B3LYP/aug-cc-pVTZ	B3LYP/6–31G(d)	3.5	0.2	2.4
MP2/cc-pVTZ	MP2/cc-pVDZ	−1.0	−4.5	2.4
BPW91/aug-cc-pVTZ	B3LYP/6–31G(d)	3.5	0.3	2.4
MP2/aug-cc-pVTZ	MP2/cc-pVDZ	−1.1	−4.6	2.5
MP3/aug-cc-pVDZ	MP2/cc-pVDZ	3.7	0.5	2.6
B3LYP/cc-pVTZ	B3LYP/cc-pVTZ	3.9	0.6	2.8
MP3/cc-pVDZ	MP2/cc-pVDZ	4.1	0.8	3.0
MP2/6–31+G(d)	MP2/cc-pVDZ	5.4	1.5	4.0
MP4/aug-cc-pVDZ	MP2/cc-pVDZ	5.4	2.4	4.4
CCSD/aug-cc-pVDZ	MP2/cc-pVDZ	5.7	2.8	4.8
CCSD(T)/cc-pVDZ	MP2/cc-pVDZ	6.0	2.9	5.0
PBE1PBE/MIDI!	PBE1PBE/MIDI!	6.7	2.8	5.3
CCSD/cc-pVDZ	MP2/cc-pVDZ	6.3	3.2	5.3
MP4/cc-pVDZ	MP2/cc-pVDZ	6.5	3.5	5.5
PBE1PBE/6–311+G(d)	B3LYP/6–31G(d)	8.1	4.4	6.8
PBE1PBE/6–31G(d)	PBE1PBE/6–31G(d)	8.1	4.7	6.9
*m*PW1PW91/6–311+G(d)	B3LYP/6–31G(d)	8.3	4.6	7.0
*m*PW1PW91/6–31G(d)	*m*PW1PW91/6–31G(d)	8.3	4.9	7.1
HF/cc-pVTZ	MP2/cc-pVDZ	8.3	5.2	7.3
HF/aug-cc-pVTZ	MP2/cc-pVDZ	8.3	5.2	7.3
HF/cc-pVDZ	HF/cc-pVDZ	9.1	5.9	8.0
B3LYP/6–311+G(d)	B3LYP/6–31G(d)	9.4	5.7	8.1
BPW91/6–311+G(d)	B3LYP/6–31G(d)	9.7	6.1	8.4
B3LYP/6–31G(d)	B3LYP/6–31G(d)	9.7	6.4	8.6
HF/aug-cc-pVDZ	MP2/cc-pVDZ	9.6	6.7	8.7
BPW91/6–31G(d)	BPW91/6–31G(d)	9.8	6.6	8.7
Relative 298 K thermal contributions	MP2/cc-pVDZ	0.6	0.7	
	mPW1PW91/cc-pVTZ	0.6	0.8	
	PBE1PBE/cc-pVTZ	0.6	0.8	
	B3LYP/cc-pVTZ	0.5	0.7	
	PBE1PBE/MIDI!	0.5	0.6	
	PBE1PBE/6–31G(d)	0.4	0.4	
	*m*PW1PW91/6–31G(d)	0.3	0.4	
	HF/cc-pVDZ	0.6	0.6	
	B3LYP/6–31G(d)	0.3	0.4	
	BPW91/6–31G(d)	0.3	0.4	

[a] Absolute energies (E_h) of **3a**: −650.73012, −642.56407, −643.97499, −643.11931, −643.11931, −643.12002, −643.97604, −644.34461, −644.34569, −642.47767, −644.34131, −643.97180, −644.40742, −642.78452, −644.38777, −642.82005, −642.56795, −644.40308, −642.48594, −642.45801, −642.63626, −642.57822, −642.53730, −640.52280, −642.49752, −642.54445, −643.93698, −643.85139, −644.30666, −644.21953, −641.68891, −641.69883, −641.60412, −644.37068, −644.35285, −641.27662, −641.630 73, −644.260 10.

provides heavy-atom bond lengths for the different tautomers computed at the MCQCISD, MP2/cc-pVDZ, and *m*PW1PW91/6–31G(d) levels. Other DFT levels of theory in general gave results sufficiently similar to *m*PW1PW91/6–31G(d) that we do not provide them here. Table 1 also provides the 298 K thermal contributions to gas-phase *free* energies relative to **3a** from various levels of theory.

There are several key trends in the data. First, Fig. 1 makes it clear that the *m*PW1PW91/6–31G(d) geometries are considerably superior to the much more expensive ones from the MP2/cc-pVDZ level. Compared with

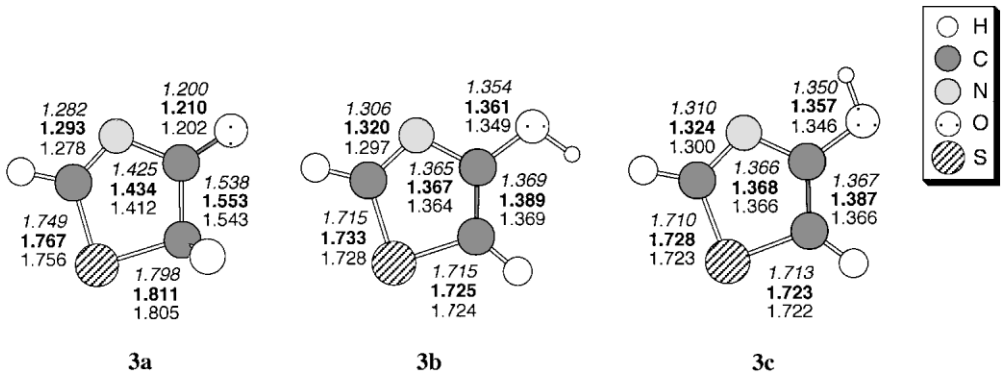

Figure 1. Heavy-atom bond lengths (Å) for **3a–c** optimized at the MCQCISD (italic), MP2/cc-pVDZ (bold) and *m*PW1PW91/6–31G(d) (roman) levels of theory

MCQCISD, all MP2 bond lengths are too long, with the average error being 0.012 Å (valence bond angles are predicted to be similar by all levels of theory and are not discussed further). The absolute error in the DFT bond lengths is only 0.006 Å, and this error is more evenly distributed between under- and overestimations. An indication of how important the geometric differences are may be had from MP2/aug-cc-pVTZ single-point energies computed for the MP2/cc-pVDZ and *m*PW1PW91/6–31G(d) geometries. The former calculation gives an error of 2.5 kcal mol^{-1}, whereas the latter has an error of only 0.2 kcal mol^{-1}. The high quality of the MP2/aug-cc-pVTZ single-point energies is similar for the other DFT geometries, reflecting their close similarities.

A separate, technical issue of some interest is the dependence of the computed relative energies on basis set quality. Comparing DFT calculations for any given functional using a consistent geometry (consistent, in this case, may effectively be taken to mean *any* DFT geometry, as they are so similar), it is apparent that highly polarized triple-ζ basis sets provide results that are very much improved over values from double-ζ sets placing only a single d function on heavy atoms (errors are reduced by an average of 5.8 kcal mol^{-1} on making this improvement in any B3LYP, *m*PW1PW91 or PBE1PBE calculation). Diffuse functions (indicated by an 'aug' or '+' in the basis set name) also improve accuracy, but by an average margin of only 0.3 kcal mol^{-1}. The near perfect accuracy of the MP2/aug-cc-pVDZ//MP2/cc-pVDZ level represents a fortuitous cancellation of errors involved with the poor geometry and the small basis set; it is not obvious that this cancellation will be maintained in the larger heterocycles. As a last technical point, we note that relative thermal contributions to 298 K free energies are computed to be the same to within 0.4 kcal mol^{-1} by every level of theory surveyed.

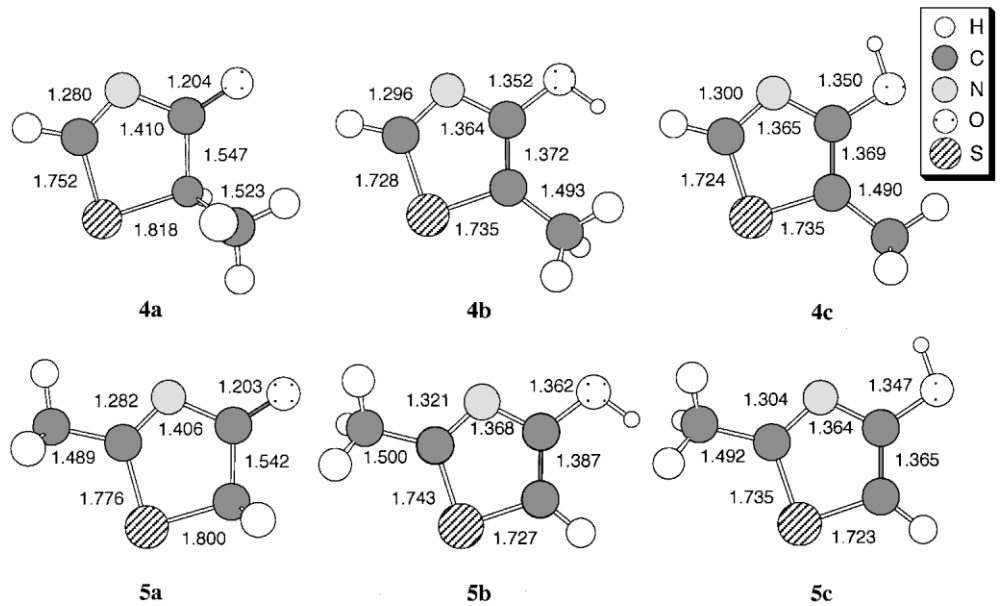

Figure 2. Heavy-atom bond lengths (Å) for **4a–c** and **5a–c** optimized at the *m*PW1PW91/6–31G(d) level of theory

Table 2. Gas-phase electronic energies (kcal mol^{-1}) relative to **4a** at various levels of theory and the relative effect of methylation

		Relative energy[a]		Relative ΔMe	
Level of theory	Geometry	**4b**	**4c**	**4b**	**4c**
PBE1PBE/aug-cc-pVTZ	*m*PW1PW91/cc-pVTZ	0.9	−3.1	−0.8	−1.5
*m*PW1PW91/aug-cc-pVTZ	*m*PW1PW91/cc-pVTZ	1.2	−2.8	−0.9	−1.6
*m*PW1PW91/cc-pVTZ	*m*PW1PW91/cc-pVTZ	1.6	−2.4	−0.8	−1.5
*m*PW1PW91/6–31G(d)	*m*PW1PW91/6–31G(d)	7.4	3.1	−0.9	−1.8

[a] Absolute energies (E_h) of **4a**: −683.665 74, −682.246 06, −682.313 78, −683.527 19.

As for the chemistry of this tautomeric equilibrium, if we sum our best estimate for 298 K thermal contributions with the MCG3//MCQCISD energies, we predict relative 298 K gas-phase free energies of 0.0, 1.8 and −1.3 kcal mol^{-1} for **3a, 3b** and **3c**, respectively. This corresponds to a roughly 1:10 mix of **3a** and **3c** at equilibrium. The preference for **3c** must reflect in part the aromaticity of the thiazole heterocycle **3c** relative to the thiazol-5(4*H*)-one species **3a**. The roughly 3.3 kcal mol^{-1} difference in energy between **3b** and **3c** computed at essentially every theoretical level, on the other hand, suggests that the nitrogen lone pair has significantly different electrostatic interactions with the hydroxyl proton (attractive in **3c**) than with the oxygen lone pairs (repulsive in **3b**). Another possibility would be differential anomeric stabilization from delocalization of oxygen lone pair density into the C(OH)═C and C(OH)—N σ^* antibonding orbitals. However, insofar as both the lengths of these two bonds are about the same in **3b** and **3c**, this suggestion is less likely.

We now consider the effects of methyl group substitution at positions 2 and 5 of the heterocycle to generate **4** and **5**, respectively. With increased size, MCQCISD optimizations become impractical. However, given the good agreement between MCQCISD and *m*PW1PW91 geometries, we anticipate that the latter will be of excellent quality for the larger heterocycles. Figure 2 provides *m*PW1PW91/6–31G(d) optimized heavy-atom bond lengths for **4** and **5**. Structures at the *m*PW1PW91/cc-pVTZ level had very similar bond lengths, to within a few thousandths of an ångstrom in most cases. Table 2 presents the relative energetic data for **4** and Table 3 for **5**. In addition to listing the relative energies, the change in energy for tautomers **a** and **b** relative to **c** compared with **3** is also tabulated, i.e. the relative effect of methylation on the individual tautomers. Thus, for instance, since the relative energies of **3a, 3b** and **3c** at the PBE1PBE/aug-cc-pVTZ//*m*PW1PW91/cc-pVTZ level are 0.0, 1.7 and − 1.6 kcal mol^{-1}, respectively, and the relative energies of **4a, 4b** and **4c** at the same level are 0.0, 0.9 and − 3.1 kcal mol^{-1}, respectively, the effect of methylation is to *stabilize* tautomers **b** and **c** relative to **a** by − 0.8 and − 1.5 kcal mol^{-1}, respectively (a negative sign reflects stabilization relative to **a** and a positive sign reflects destabilization relative to **a**). We restrict ourselves to DFT models from this point on since MP2 calculations with triple-ζ basis sets, even as single points, quickly become impractical with increasing size of the heterocycles.

The PBE1PBE and *m*PW1PW91 functionals agree closely with one another for relative energies when a large basis set is used (note that diffuse functions, however, do not appear to be important). The energies at the *m*PW1PW91/6–31G(d) level, however, suffer from an overstabilization of the keto tautomer relative to the other two, just as was the case for **3**. However, the effects of methylation are very consistently predicted irrespective of the basis set size. Thus, all levels predict that the hydroxyl tautomers are stabilized by 5-methyl substitution relative to the keto tautomer by about 1.5 kcal mol^{-1} for **4c** and slightly less than 1 kcal mol^{-1} for **4b** (where there is a steric clash between the hydroxyl proton and the 5-methyl group). With respect to *free* energies, the *m*PW1PW91/cc-pVTZ calculations predict thermal contributions to 298 K free energies to be − 0.3 and − 0.1 kcal mol^{-1} for **4b** and **4c**, respectively, relative to **4a**. Noting that these same relative thermal contributions in **3** were 0.6 and 0.8 (see Table 1), we may again express this in terms of a methylation effect, in which case the hydroxyl tautomers are stabilized in a free energy sense

Table 3. Gas-phase electronic energies (kcal mol^{-1}) relative to **5a** at various levels of theory and the relative effect of methylation

		Relative energy[a]		Relative ΔMe	
Level of theory	Geometry	**5b**	**5c**	**5b**	**5c**
PBE1PBE/aug-cc-pVTZ	*m*PW1PW91/cc-pVTZ	4.5	1.4	+2.8	+3.0
*m*PW1PW91/aug-cc-pVTZ	*m*PW1PW91/cc-pVTZ	4.8	1.6	+2.7	+2.8
*m*PW1PW91/cc-pVTZ	*m*PW1PW91/cc-pVTZ	5.0	1.8	+2.6	+2.7
*m*PW1PW91/6–31G(d)	*m*PW1PW91/6–31G(d)	10.8	7.5	+2.5	+2.6

[a] Absolute energies (E_h) of **5a**: −683.676 39, −682.252 97, −682.321 08, −683.537 04.

Table 4. Best-estimate relative 298 K gas-phase free energies (kcal mol^{-1}) for tautomers

	Energy relative to tautomer **a**										
Heterocycle	**b**	**c**	**d**	**e**	**f**	**g**	**h**	**i**	**j**	**k**	**l**
3[a]	1.8	−1.3									
4[b]	0.0	−3.8									
5[b]	3.6	0.5									
6[b]	2.4	−0.8	4.5	6.5	3.0						
7[b]	2.4	−0.5	4.6	6.0	3.0	−0.1	2.4	−0.5	4.5	6.2	3.0

[a] Sum of MCG3//MCQCISD energies and mPW1PW91/cc-pVTZ 298 K thermal contributions.
[b] Sum of substitution effects on relative energies and relative 298 K thermal contributions computed at the mPW1PW91/aug-cc-pVTZ//mPW1PW91/cc-pVTZ added to relative tautomer energies for **3**.

by 5-methyl substitution relative to the keto tautomer by about 2.5 kcal mol^{-1} for **4c** and 1.8 kcal mol^{-1} for **4b**. This roughly 2 kcal mol^{-1} stabilization is entirely consistent with the expected energetic preference deriving from the formal C═C double bond in **4b** and **4c** being more highly substituted.[29]

If we continue in the vein of using a perturbational analysis to modify our best estimates for relative free energies, we may add the above computed stabilization free energies to our MCG3 estimate for the parent tautomeric equilibrium, in which case we predict relative 298 K gas-phase free energies of 0.0, 0.0 and −3.8 kcal mol^{-1} for **4a, 4b** and **4c**, respectively. These values are listed in Table 4.

For heterocycle **5**, the performances of the theoretical levels follow the same trends as for **4**: relative tautomer energies computed using large basis sets do not agree well with those computed using smaller ones, but relative methylation effects agree closely. In this case, methylation of the 2 position stabilizes the keto tautomer relative to the hydroxyl tautomers by slightly less than 3 kcal mol^{-1}. From a chemical standpoint, we may understand this by adopting a resonance picture for the keto tautomer, as illustrated.

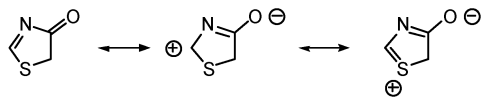

Methylation at the 2-position stabilizes cationic charge development at this position (the middle mesomer). To the extent that this modifies the valence-bond description of the keto tautomer to include more zwitterionic character, we would expect the C(O)—N bond to be shorter in **5a** than in **3a** and the C(H)—N and C═O bonds to be longer in **5a** than in **3a**, and this is precisely what is observed in the optimized geometries, although the magnitudes of these changes are fairly small. With respect to *free* energies, the *m*PW1PW91/cc-pVTZ calculations predict thermal contributions to 298 K free energies to be − 0.3 and − 0.2 kcal mol^{-1} for **5b** and **5c**, respectively, relative to **5a**. Following the same perturbational approach outlined above for **4**, we predict as our best estimate relative 298 K gas-phase free energies of 0.0, 3.6 and 0.5 kcal mol^{-1} for **5a, 5b** and **5c**, respectively (Table 4).

When the 2-substituent is changed from a methyl group to a 2′-thiazole, geometric analysis suggests that

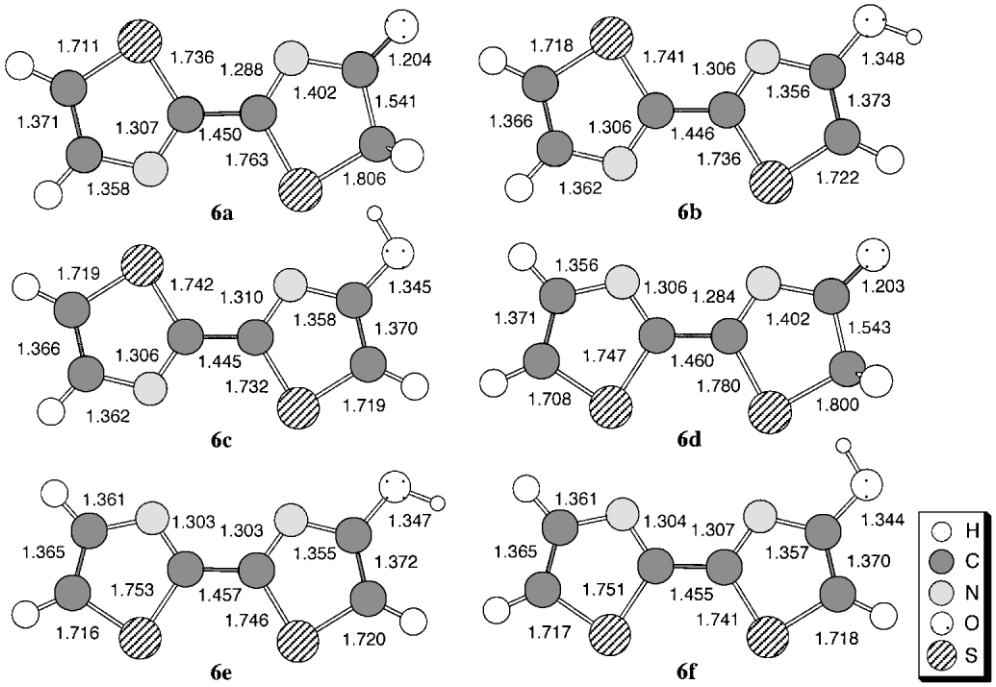

Figure 3. Heavy-atom bond lengths (Å) for **6a–f** optimized at the *m*PW1PW91/6–31G(d) level of theory

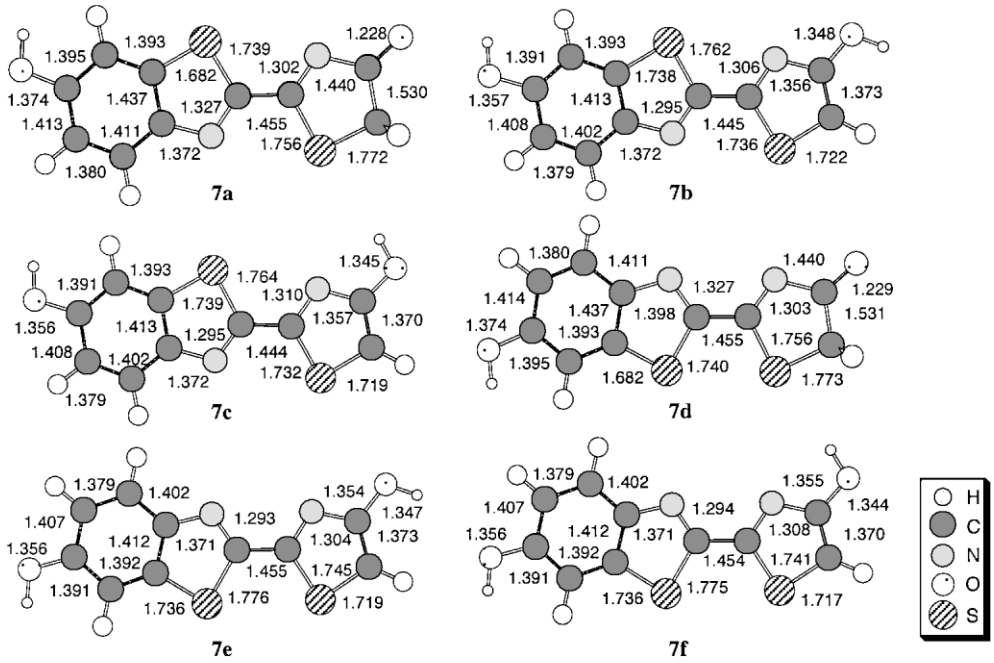

Figure 4. Heavy-atom bond lengths (Å) for **7a–f** optimized at the *m*PW1PW91/6–31G(d) level of theory. Note that isomers **7g–l** correspond to **7a–f** in all respects except for rotation of the phenolic hydroxyl; geometric data for these alternative phenolic rotamers do not differ significantly from those shown

the heterocycle is better at stabilizing the charge separated mesomer, through conjugation, than is a methyl group, through hyperconjugation. Thus, in **6a**, the C(O)—N bond is even shorter than in **5a**, and the C(H)—N and C═O bonds are even longer (Fig. 3). However, the net stabilization of the keto tautomer relative to the hydroxyls by virtue of this substitution is reduced (Table 5), from slightly less than 3 kcal mol^{-1} in **5** to slightly less than 1 kcal mol^{-1} in **6**. This may be related to increased repulsive interactions between the S and N lone pairs resulting from the much shorter C(S)—N bond in **6a** than in **6b** or **6c**, but this is speculative.

With respect to rotational isomerism about the 2,2′ bond, all levels of theory indicate that the syn rotamer is disfavored by between 5 and 6 kcal mol^{-1} (comparing equivalent bisthiazole tautomers). The largest destabilization is associated with the keto tautomer, again possibly because of the short C(S)—N bond and further increased lone pair–lone pair repulsive interactions.

Relative to the parent system, at the *m*PW1PW91/cc-pVTZ level the differential thermal contributions to 298 K free energies relative to **6a** arising from thiazole substitution are predicted to be 0.0, −0.4, −1.3, −1.5 and − 1.0 kcal mol^{-1} for **6b–f**, respectively. When these differential thermal contributions are summed with the best thiazole substitution effects in Table 5 and the MCG3//MCQCISD energies for the parent system, we predict as best-estimate relative 298 K gas-phase free energies 0.0, 2.4, −0.8, 4.5, 6.5 and 3.0 kcal mol^{-1} for **6a–f**, respectively (Table 4).

Benzannelation of the unsubstituted thiazole ring has only a very small effect on the tautomerism of the luciferin heterocycle **7** compared with **6**: all substitution effects relative to parent system **3** are the same for **7** and **6** to within 0.5 kcal mol^{-1} (Table 6). Equivalent tautomers differing only as hydroxyl rotamers have identical electronic energies to within 0.1 kcal mol^{-1}, so relative energies for **7g–l** are not tabulated separately (although

Table 5. Gas-phase electronic energies (kcal mol^{-1}) relative to **6a** at various levels of theory and the relative effect of substitution by 2′-thiazolyl

		Relative energy[a]					Relative Δthiazole				
Level of theory	Geometry	**b**	**c**	**d**	**e**	**f**	**b**	**c**	**d**	**e**	**f**
*m*PW1PW91/aug-cc-pVTZ	*m*PW1PW91/cc-pVTZ	2.7	−0.3	5.8	8.5	4.6	+0.6	+0.9	+5.8	+6.4	+5.8
*m*PW1PW91/cc-pVTZ	*m*PW1PW91/cc-pVTZ	3.0	−0.2	6.0	8.8	4.9	+0.6	+0.7	+6.0	+6.4	+5.8
*m*PW1PW91/6–31G(d)	*m*PW1PW91/6–31G(d)	8.6	5.3	6.6	15.2	11.0	+0.3	+0.4	+6.6	+6.9	+6.1

[a] Absolute energies (E_h) of **6a**: −1212.26931, −1212.26327, −1212.05351.

Table 6. Gas-phase electronic energies (kcal mol^{-1}) relative to **7a** at various levels of theory and the relative effect of substitution by 2′-(6-hydroxybenzothiazolyl)

		Relative energy[a]					Relative Δbenzothiazole				
Level of theory	Geometry	**b**	**c**	**d**	**e**	**f**	**b**	**c**	**d**	**e**	**f**
*m*PW1PW91/aug-cc-pVTZ	*m*PW1PW91/6–31G(d)	2.8	−0.3	5.7	7.9	4.1	+0.7	+0.9	+5.7	+5.9	+5.3
*m*PW1PW91/6–31G(d)	*m*PW1PW91/6–31G(d)	8.5	5.2	6.6	14.9	10.8	+0.2	+0.3	+6.6	+6.6	+5.8

[a] Absolute energies (E_h) of **7a**: −1441.174 21, −1440.870 80.

they are properly accounted for in Table 4 and in Boltzmann-averaged free energies discussed further below).

Relative to the parent system, at the *m*PW1PW91/6–31G(d) level the differential thermal contributions to 298 K free energies relative to **7a** arising from thiazole substitution are predicted to be −0.1, −0.1, −1.1, −1.7 and −1.0 kcal mol^{-1} for **7b–f**, respectively. When these differential thermal contributions are summed with the best thiazole substitution effects in Table 5 and the MCG3//MCQCISD energies for the parent system, we predict as best-estimate relative 298 K gas-phase free energies 0.0, 2.4, −0.5, 4.6, 6.0 and 3.0 kcal mol^{-1} for **7a–f**, respectively (Table 4).

Deprotonation of luciferin

Relative to **3a**, the energy required to generate $\mathbf{3}^-$ is predicted to be 355.1 kcal mol^{-1} at all three of the levels MCG3//MCQCISD, *m*PW1PW91/aug-cc-pVTZ, and *m*PW1PW91/aug-cc-pVTZ//*m*PW1PW91/6–31G(d). Adding 298 K thermal contributions, the free energy of deprotonation is predicted to be 339.2 kcal mol^{-1}. Given the perfect agreement between these various levels of theory for **3**, we chose to apply the most economical, *m*PW1PW91/aug-cc-pVTZ//*m*PW1PW91/6–31G(d), to **7**. The results are given in Table 7, and indicate that the anion $^-$**7a** completely dominates at equilibrium. This is readily understood from consideration of the resonance delocalization available to the keto tautomer, but not the hydroxyl tautomers, when the phenol is deprotonated, as illustrated.

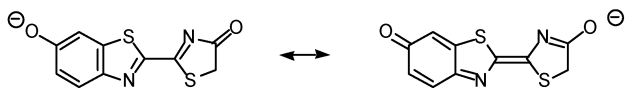

Invocation of this resonance is supported by the substantially shorter C2—C2′ bond in $^-$**7a** (1.407 Å) than in any of the other isomers (typically 1.42–1.44 Å). No special resonance is available to the tautomers involving deprotonation of the non-benzannelated thiazole ring, and these species are predicted to be correspondingly much higher in energy.

The trend with respect to rotation about the heterocycle–heterocycle bond is about the same in both sets of anions as in the neutrals, i.e. there is a roughly 6 kcal mol^{-1} preference not to have equivalent heteroatoms syn to one another.

Aqueous solvation effects

Absolute solvation free energies at the SM5.42R/BPW91/6–31G(d)//*m*PW1PW91/6–31G(d) level for all molecules discussed thus far are listed in Table 8. Relative tautomer free energies in aqueous solution, derived from summing the relative solvation free energies with the relative gas-phase free energies, are listed in Table 9. Table 10 compares the results from Tables 4 and 9 expressed in terms of tautomer percentage contributions to the full equilibrium population.

There are several trends worthy of note in the solvation data. First, solvation tends to level relative molecular energies, since in the gas phase more polar molecules tend to be less stable, but such molecules are precisely those that are better solvated. Thus, in every instance, hydroxyl tautomer **b** is better solvated than keto tautomer **a** by 1–3 kcal mol^{-1}. Thus, the populations of tautomers **a** and **b** always shift in aqueous solution to reduce the ratio of **a** to **b**. With respect to hydroxyl rotation, again, solvent levels the gas-phase preference for the hydroxyl proton to be oriented into space near the nitrogen lone pair. Thus, the gas-phase preference for **c** over **b** is reduced substantially; indeed, in **6** and **7** the preference inverts, and more of tautomer **b** is present in aqueous solution than of tautomer **c** (in the case of **7**, this is true irrespective of the phenol hydroxyl orientation). In the case of **3** and **5**, the free energies of the two tautomers in aqueous solution are predicted to be degenerate, and only in the case of **4**, where there is a steric clash in tautomer **b**, does **c** remain the dominant species.

Table 7. Gas-phase electronic and 298 K free energies (kcal mol^{-1}) relative to $^-$**7a** at the *m*PW1PW91/aug-cc-pVTZ//*m*PW1PW91/6–31G(d) level of theory[a]

Quantity	$^-$**7b**	$^-$**7c**	$^-$**7d**	$^-$**7e**	$^-$**7f**	**7a**$^-$	**7d**$^-$	**7g**$^-$	**7j**$^-$
E	14.1	9.8	5.0	18.6	14.1	16.9	22.5	17.2	22.5
$G°_{298}$	13.9	9.8	4.6	18.0	13.8	16.6	22.6	16.8	22.6

[a] Absolute energy (E_h) of $^-$**7a**: −1440.648 66 (thermal contribution 0.094 89).

Table 8. 298 K aqueous solvation free energies (kcal mol^{-1}) for tautomers at the SM5.42R/BPW91/6–31G(d)//*m*PW1PW91/6–31G(d) level

	a	b	c	d	e	f	g	h	i	j	k	l
3	−12.4	−13.7	−10.6									
4	−10.7	−13.0	−9.9									
5	−11.8	−13.4	−10.3									
6	−17.4	−19.5	−15.6	−16.0	−18.0	−14.8						
7	−23.8	−24.7	−21.3	−25.3	−25.8	−22.0	−23.5	−24.4	−21.2	−25.3	−25.8	−21.9
$^{-}$**7**	−55.9	−65.4	−60.2	−56.6	−65.4	−60.5						
7^{-}	−70.4			−72.0			−70.9			−72.2		

Table 9. Best-estimate relative 298 K aqueous free energies (kcal mol^{-1}) for tautomers[a]

	Energy relative to tautomer **a**										
Heterocycle	**b**	**c**	**d**	**e**	**f**	**g**	**h**	**i**	**j**	**k**	**l**
3	0.5	0.5									
4	−2.3	−3.0									
5	2.0	2.0									
6	0.3	1.0	5.9	5.9	5.6						
7	1.5	2.0	3.1	4.0	4.8	0.2	1.8	2.1	3.0	4.2	4.9
	$^{-}$**7b**	$^{-}$**7c**	$^{-}$**7d**	$^{-}$**7e**	$^{-}$**7f**	**7a**$^{-}$	**7d**$^{-}$	**7g**$^{-}$	**7j**$^{-}$		
$^{-}$**7** and **7**$^{-}$	4.3	0.3	17.3	4.3	9.2	2.1	6.5	1.8	6.3		

[a] Sum of relative gas-phase free energies in Table 4 or 7 and relative aqueous free energies of solvation determined from data in Table 8.

Another interesting observation is the sensitivity of the solvation free energy to the position of the methyl group in heterocycles **4** and **5**. The solvation free energies for equivalent hydroxyl tautomers (**b** and **c**) differ by only 0.4 kcal mol^{-1} across these two systems, suggesting that the descreening of polar functionality by the methyl group is about the same independent of its position on the ring. However, tautomer **a** is 1.1 kcal mol^{-1} better solvated in **5** than in **4**, supporting the contention above that substitution at the 5 position increases the weight of the zwitterionic mesomer, which would be expected to have a very large, negative solvation free energy, in the valence-bond depiction of the keto structure.

The leveling effect of solvent is particularly noticeable in the case of the luciferin anion. Since tautomer $^{-}$**7a** owes much of its special gas-phase stability to its ability to delocalize negative charge, as discussed above, it is poorly solvated compared with other tautomers, where concentrated charge is favorably disposed to interact strongly with surrounding solvent. Thus, although tautomer $^{-}$**7a** completely dominates the equilibrium population in the gas phase, in aqueous solution the anion derived from deprotonation of the thiazolone is present to the extent of 4.7% at equilibrium (summing over both phenol hydroxyl rotamers), and the **c** tautomer of the phenolate also grows in to a 35.9% extent.

Table 10. 298 K tautomer populations (%) in the gas phase and aqueous solution[a]

	a	b	c	d	e	f	g	h	i	j	k	l
3	10.2	0.5	89.3									
	53.6	23.2	23.2									
4	0.2	0.2	99.7									
	0.5	23.6	75.9									
5	69.6	0.2	30.2									
	93.4	3.3	3.3									
6	20.7	0.4	78.8	0.0	0.0	0.1						
	55.8	33.8	10.5	0.0	0.0	0.0						
7	14.6	0.3	33.7	0.0	0.0	0.1	17.3	0.3	33.7	0.0	0.0	0.1
	51.9	4.2	1.8	0.3	0.1	0.0	37.2	2.6	1.5	0.3	0.0	0.0
	$^{-}$**7a**	$^{-}$**7b**	$^{-}$**7c**	$^{-}$**7d**	$^{-}$**7e**	$^{-}$**7f**	**7a**$^{-}$	**7d**$^{-}$	**7g**$^{-}$	**7j**$^{-}$		
$^{-}$**7** and **7**$^{-}$	100	0.0	0.0	0.0	0.0	0.0	0.0	0.0	0.0	0.0		
	59.3	0.0	35.9	0.0	0.0	0.0	1.8	0.0	2.9	0.0		

[a] From free energies in Tables 4, 7 and 9; gas-phase values above, solution values below.

Prediction of oxyluciferin pK_a values

Computation of pK_a may be accomplished in a direct fashion by computing the free energy change ΔG° for deprotonation in aqueous solution (1 molar standard state) and then using

$$pK_a = \Delta G^\circ / 2.303RT \quad (1)$$

where R is the universal gas constant and T is the absolute temperature. Because both the neutral and anionic forms of oxyluciferin are speciated over a number of tautomers, we must employ a population-averaged free energy. This may be computed as

$$G^\circ = -RT \ln \sum_i e^{-G_i^\circ/RT} \quad (2)$$

where i runs over all tautomers. In this case, a tautomer free energy is defined as the electronic energy at the *m*PW1PW91/aug-cc-pVTZ//*m*PW1PW91/6–31G(d) level plus 298 K thermal contributions (using a 1 molar standard state concentration) plus the free energy of aqueous solvation from the SM5.42R level. For the proton itself, the electronic energy is zero, and both the thermal contribution and solvation free energy are available from experiment.[67] Thus, we have for the neutral species an aqueous free energy of $-1441.101\ 92$ E_h, for the anion $-1440.640\ 40$ E_h, and for the proton $-0.430\ 04$ E_h. Using these quantities in Eqn. (1) leads to a free energy change of 19.8 kcal mol^{-1}, which corresponds to a raw pK_a value of 14.3. This value is not physically realistic, and simply reflects the difficulty of computing a raw pK_a value from first principles.

We may improve on this estimate, however, by considering the same procedure for 2-naphthol, which is a reasonably analogous phenolic species having a known pK_a of 9.5.[68] The raw pK_a value that is computed from the identical procedure to that just described above for luciferin is 17.3. Thus, we may take advantage of error cancellation by noting that theory predicts luciferin to have a first pK_a value that is 3 units lower than for 2-naphthol, and adding this difference to the experimental 2-naphthol value. Thus, we predict as our best estimate a first pK_a of 6.5 for luciferin. As already noted above, the deprotonated species is an equilibrium mixture, about 95% of which is in a phenolate form, i.e. one may say that the phenolic proton is more acidic than the thiazolone proton. Indeed, we could use the relative free energies of the two subpopulations to assign a pseudo-pK_a value of about 5.2 to the thiazolone/hydroxythiazole moiety (i.e. this pK_a is associated with the hypothetical process of deprotonating this heterocycle while the phenol functionality is still intact). We have not attempted to calculate an actual *second* pK_a, as the computational uncertainties associated with dianions grow fairly large, and good models for error correction are less available.

CONCLUSIONS

Converged prediction of tautomer energies in the parent thiazol-5(4*H*)-one/5-hydroxythiazole system requires the application of very complete levels of electronic structure theory. Results accurate to within 1 kcal mol^{-1} of converged quantum mechanical predictions, however, may be obtained from DFT calculations using basis sets of triple-ζ quality. Accurate geometries are more readily obtained, with those from DFT calculations using basis sets of double-ζ quality being as good as those from the much more computationally demanding MCQCISD level.

In the gas phase, the 5-hydroxythiazole tautomer is predicted to be preferred over the thiazol-5(4*H*)-one tautomer unless a good conjugative or hyperconjugative donor is substituted at position **2**, in which position it stabilizes a zwitterionic mesomer of the system. Substitution at position **4**, on the other hand, further stabilizes hydroxythiazole tautomers since it adds to the stability of the double bond between the 4 and 5 positions. In most cases, however, the preferences for the dominant tautomer are quantitatively small, so that mixtures of readily detectable quantities of multiple tautomers are predicted for every case except 5-hydroxy-4-methylthiazole.

Solvation effects are predicted to level the energetic differences between tautomers, and in general to favor the keto tautomer over hydroxyl tautomers, again owing to the contribution of the very polar zwitterionic mesomer to a valence bond description of the former. This effect reverses the gas-phase trend in terms of which tautomer is generally dominant, but does not do so to as large an extent as mixtures do not continue to be predicted for most cases.

Applying a strategy of combining gas-phase calculations with a continuum model for aqueous solvation, oxyluciferin is predicted to have a pK_a that is 3 units more acidic than 2-naphthol, which corresponds to a value of 6.5. The deprotonated oxyluciferin anion also exists as an equilibrium mixture of tautomers, but phenolate tautomers dominate over those derived from deprotonation of the hydroxythiazole by a factor of about 20:1.

Firmly anchoring the relative energetics of the different neutral and anionic tautomers of oxyluciferin should prove useful in predicting the corresponding relative energies of the first excited singlet state. Calculations along these lines will be reported in due course.

Acknowledgements

E.D. received support from the National Science Foundation under Grant No. NSF/CHE-0137438 (REU Site Award). We thank Ed Sherer for helpful discussions about luciferin and Bethany Kormos for technical assistance in using MULTILEVEL.

REFERENCES

1. Seliger HH, McElroy WD. *Proc. Natl. Acad. Sci. USA* 1964; **52**: 75–81.
2. Seliger HH, Morton RA. In *Photophysiology*, vol. **4**, Giese AC (ed). Academic Press: New York, 1968; 253–314.
3. White EH, Rapaport E, Seliger HH, Hopkins TA. *Bioorg. Chem.* 1971; **1**: 92–122.
4. Suzuki N, Gogo T. *Tetrahedron* 1972; **28**: 4075–4082.
5. DeLuca M, McElroy WD. *Methods Enzymol*. 1978; **57**: 3–36.
6. White EH, Steinmetz MG, Miano JD, Wildes PD, Morland R. *J. Am. Chem. Soc.* 1980; **102**: 3199–3208.
7. Schuster GB, Schmidt SP. *Adv. Phys. Org. Chem.* 1982; **18**: 187–238.
8. McCapra F, Gilfoyle DJ, Young DW, Church NJ, Spencer P. In *Bioluminescence and Chemiluminescence*, Campbell AK, Kricka LJ, Stanley PE (eds). Wiley: New York, 1994; 387–391.
9. Wood KV. *Photochem. Photobiol.* 1995; **62**: 662–673.
10. Usami K, Isobe M. *Tetrahedron* 1996; **52**: 12061–12090.
11. McCapra F. In *Bioluminescence and Chemiluminescence*, Hastings JW, Kricka LJ, Stanley PE (eds). J Wiley: New York, 1997; 7–15.
12. Wilson T, Hastings JW. *Annu. Rev. Cell Biol.* 1998; **14**: 197–230.
13. Takano Y, Tsunesada T, Isobe H, Yoshioka Y, Yamaguchi K, Saito I. *Bull. Chem. Soc. Jpn.* 1999; **72**: 213–225.
14. McCapra F. *Methods Enzymol.* 2000; **305**: 3–47.
15. Biggley WH, Lloyd JE, Seliger HH. *J. Gen. Phys.* 1967; **50**: 1681–1692.
16. Wood KV. *J. Biolum. Chemilum.* 1990; **5**: 107–114.
17. Kajiyama N, Nakano E. *Protein Eng.* 1991; **4**: 691–693.
18. White EH, Roswell DF. *Photochem. Photobiol.* 1991; **53**: 131–136.
19. Gandelman OA, Brovko LY, Ugarova NN, Chikishev AY, Shkurimov AP. *J. Photochem. Photobiol. B* 1993; **19**: 187–191.
20. Hastings JW. *Gene* 1996; **173**: 5–11.
21. Branchini BR, Murtiashaw MH, Magyar RA, Portier NC, Ruggiero MC, Stroh JG. *J. Am. Chem. Soc.* 2001; **124**: 2112–2113.
22. White EH, Wörther H, Field GF, McElroy WD. *J. Org. Chem.* 1965; **30**: 2344–2348.
23. White EH, Wörther H, Seliger HH, McElroy WD. *J. Am. Chem. Soc.* 1966; **88**: 2015–2019.
24. Branchini BR, Magyar RA, Murtiashaw MH, Portier NC. *Biochemistry* 2001; **40**: 2410–2418.
25. Kwiatkowski JS, Zielinski TJ, Rein R. *Adv. Quantum Chem.* 1986; **18**: 85–130.
26. Karelson MM, Katritzky AR, Szafran M, Zerner MC. *J. Org. Chem.* 1989; **54**: 6030–6034.
27. Leszczynski J. *Chem. Phys. Lett.* 1990; **174**: 347–354.
28. Cramer CJ, Truhlar DG. *J. Am. Chem. Soc.* 1991; **113**: 8552–8553.
29. Cramer CJ, Truhlar DG. *J. Am. Chem. Soc.* 1993; **115**: 8810–8817.
30. Cramer CJ, Truhlar DG. In *Solvent Effects and Chemical Reactivity*, Tapia O, Bertrán J (eds). Kluwer: Dordrecht, 1996; 1–81.
31. Hernández B, Orozco M, Luque FJ. *J. Comput.-Aided Mol. Des.* 1997; **11**: 153–162.
32. Luque FJ, López-Bes JM, Cemeli J, Aroztegui M, Orozco M. *Theor. Chem. Acc.* 1997; **96**: 105–113.
33. Sherer EC, Cramer CJ. *J. Comput. Chem.* 2001; **22**: 1167–1179.
34. Mennucci B, Toniolo A, Tomasi J. *J. Phys. Chem.* 2001; **105**: 4749–4757.
35. Jang YH, Goddard WA, Noyes KT, Sowers LC, Hwang S, Chung DS. *Chem. Res. Toxicol.* 2002; **15**: 1023–1035.
36. Pullman B, Pullman A. *Adv. Heterocycl. Chem.* 1971; **13**: 77–136.
37. Topal MD, Fresco JR. *Nature (London)* 1976; **263**: 285–287.
38. Bashford D, Karplus M. *Biochemistry* 1990; **29**: 10219–10225.
39. Schüürmann G. *Quant. Struct.–Act. Relat.* 1996; **15**: 121–132.
40. Topol IA, Tawa GJ, Burt SK, Rashin AA. *J. Phys. Chem. A* 1997; **101**: 10075–10081.
41. Cramer CJ, Truhlar DG. *Chem. Rev.* 1999; **99**: 2161–2200.
42. Richardson WH, Peng C, Bashford D, Noodleman L, Case DA. *Int. J. Quantum Chem.* 1997; **61**: 207–217.
43. Liptak MD, Gross KC, Seybold PG, Feldgus S, Shields GC. *J. Am. Chem. Soc.* 2002; **124**: 6421–6427.
44. Klicic JJ, Friesner RA, Liu SY, Guida WC. *J. Phys. Chem. A* 2002; **106**: 1327–1335.
45. Chipman DM. *J. Phys. Chem. A* 2002; **106**: 7413–7422.
46. Cramer CJ. *Essentials of Computational Chemistry: Theories and Models.* Wiley: Chichester, 2002; pp 319–345.
47. Perdew J, Wang Y. *Phys. Rev. B* 1992; **45**: 13244–13249.
48. Burke K, Ernzerhof M, Perdew JP. *Chem. Phys. Lett.* 1997; **265**: 115–120.
49. Burke K, Perdew JP, Wang Y. In *Electronic Density Functional Theory. Recent Progress and New Directions*, Dobson JF, Vignale G, Das MP (eds). Plenum Press: New York, 1998; 81–121.
50. Adamo C, Barone V. *J. Chem. Phys.* 1998; **108**: 664–675.
51. Hehre WJ, Radom L, Schleyer PvR, Pople JA. *Ab Initio Molecular Orbital Theory.* Wiley: New York, 1986.
52. Fast PL, Truhlar DG. *J. Phys. Chem. A* 2000; **104**: 6111–6116.
53. Tratz CM, Fast PL, Truhlar DG. *Phys. Chem. Commun.* 1999; **2**: Article 14.
54. Fast PL, Sanchez ML, Truhlar DG. *Chem. Phys. Lett.* 1999; **306**: 407–410.
55. Koch W, Holthausen MC. *A Chemist's Guide to Density Functional Theory.* Wiley-VCH: Weinheim, 2000.
56. Easton RE, Giesen DJ, Welch A, Cramer CJ, Truhlar DG. *Theor. Chim. Acta* 1996; **93**: 281–301.
57. Dunning TH. *J. Chem. Phys.* 1989; **90**: 1007–1023.
58. Kendall RA, Dunning TH, Harrison RJ. *J. Chem. Phys.* 1992; **96**: 6796–6806.
59. Woon DE, Dunning TH. *J. Chem. Phys.* 1993; **98**: 1358–1371.
60. Curtiss LA, Raghavachari K, Redfern PC, Rassolov V, Pople JA. *J. Chem. Phys.* 1998; **109**: 7764–7780.
61. Zhu T, Li J, Hawkins GD, Cramer CJ, Truhlar DG. *J. Chem. Phys.* 1998; **109**: 9117–9133.
62. Li J, Zhu T, Cramer CJ, Truhlar DG. *J. Phys. Chem. A* 1998; **102**: 1820–1831.
63. Frisch MJ, Trucks GW, Schlegel HB, Scuseria GE, Robb MA, Cheeseman JR, Zakrzewski VG, Montgomery JA, Stratmann RE, Burant JC, Dapprich S, Millam JM, Daniels AD, Kudin KN, Strain MC, Farkas O, Tomasi J, Barone V, Cossi M, Cammi R, Mennucci B, Pomelli C, Adamo C, Clifford S, Ochterski J, Petersson GA, Ayala PY, Cui Q, Morokuma K, Salvador P, Dannenberg JJ, Malick DK, Rabuck AD, Raghavachari K, Foresman JB, Cioslowski J, Ortiz JV, Baboul AG, Stefanov BB, Liu G, Liashenko A, Piskorz P, Komaromi I, Gomperts R, Martin RL, Fox DJ, Keith T, Al-Laham MA, Peng CY, Nanayakkara A, Challacombe M, Gill PMW, Johnson B, Chen W, Wong MW, Andres JL, Gonzalez C, Head-Gordon M, Replogle ES, Pople JA. Gaussian 98 (Revision A.10). Gaussian: Pittsburgh, PA, 2001.
64. Xidos JD, Li J, Thompson JD, Hawkins GD, Winget PD, Zhu T, Rinaldi D, Liotard DA, Cramer CJ, Truhlar DG, Frisch MJ. MN-GSM, Version 1.8. University of Minnesota: Minneapolis, MN, 2001.
65. Rodgers JM, Lynch BJ, Fast PL, Chuang Y-Y, Pu J, Truhlar DT. MULTILEVEL. University of Minnesota: Minneapolis, MN, 2000.
66. Kormos BL, Cramer CJ. *J. Phys. Org. Chem.* 2002; **15**: 712–720.
67. Lewis A, Bumpus JA, Truhlar DG, Cramer CJ. *J. Chem. Educ.* submitted for publication.
68. Lide DR (ed). *CRC Handbook of Chemistry and Physics*. CRC Press: Boca Raton, FL, 1995; section 8, p 64.